HHS Public Access

Author manuscript

Exp Eye Res. Author manuscript; available in PMC 2024 September 27.

Published in final edited form as:

Exp Eye Res. 2022 February ; 215: 108930. doi:10.1016/j.exer.2022.108930.

Mesenchymal stem cell secretome protects against oxidative stress-induced ocular blast visual pathologies

Kumar Abhiram Jha[a,1,2], **Pratheepa Kumari Rasiah**[a,1], **Jordy Gentry**[a], **Nobel A. Del Mar**[b], **Ravi Kumar**[c], **Adebowale Adebiyi**[c], **Anton Reiner**[d], **Rajashekhar Gangaraju**[e,*]

[a]Department of Ophthalmology, University of Tennessee Health Science Center, 930 Madison Ave, Suite 769, Memphis, TN, 38163, USA

[b]Department of Anatomy & Neurobiology, University of Tennessee Health Science Center, 317 Wittenborg Building, 875 Monroe Avenue, Memphis, TN, 38163, USA

[c]Department of Physiology, University of Tennessee Health Science Center, 956 Court Avenue, Coleman Building, Suite C211, Memphis, TN, 38163, USA

[d]Department of Anatomy & Neurobiology, University of Tennessee Health Science Center, 522 Wittenborg Building, 875 Monroe Avenue, Memphis, TN, 38163, USA

[e]Department of Ophthalmology, Anatomy & Neurobiology, Neuroscience Institute, University of Tennessee Health Science Center, 930 Madison Ave, Suite 768, Memphis, TN, 38163, USA

Abstract

Visual deficits are a common concern among subjects with head trauma. Stem cell therapies have gained recent attention in treating visual deficits following head trauma. Previously, we have shown that adipose-derived stem cell (ASC) concentrated conditioned medium (ASC-CCM), when delivered via an intravitreal route, yielded a significant improvement in vision accompanied by a decrease in retinal neuroinflammation in a focal cranial blast model that indirectly injures the retina. The purpose of the current study is to extend our previous studies to a direct ocular blast injury model to further establish the preclinical efficacy of ASC-CCM. Adult C57BL/6J mice were subjected to repetitive ocular blast injury (rOBI) of 25 psi to the left eye, followed by intravitreal delivery of ASC-CCM (~200 ng protein/2 μl) or saline within 2–3 h. Visual function and histological changes were measured 4 weeks after injury and treatment. *In vitro*, Müller cells were used to evaluate the antioxidant effect of ASC-CCM. Visual acuity, contrast sensitivity, and b-wave amplitudes in rOBI mice receiving saline were significantly decreased compared with age-matched sham blast mice. Immunohistological analyses demonstrated a significant increase in glial fibrillary acidic protein (a retinal injury marker) in Müller cell processes, DNA/RNA damage, and nitrotyrosine (indicative of oxidative stress) in the retina, while qPCR analysis revealed a

*Corresponding author. sgangara@uthsc.edu (R. Gangaraju).

[2]Present Address- GIOSTAR Research Inc. Pvt. Ltd, Mohali, Punjab, India.

[1]Equal contribution.

Declaration of competing interest

RG is a co-founder and holds equity in Cell Care Therapeutics Inc., whose interest is in using adipose-derived stromal cells in visual disorders. None of the other authors declare any financial conflicts.

Appendix A. Supplementary data

Supplementary data to this article can be found online at https://doi.org/10.1016/j.exer.2022.108930.

>2-fold increase in pro-inflammatory cytokines (TNF-α, ICAM1, and Ccl2) in the retina, as well as markers for microglia/macrophage activation (IL-1β and CD86). Remarkably, rOBI mice that received ASC-CCM demonstrated a significant improvement in visual function compared to saline-treated rOBI mice, with visual acuity, contrast sensitivity, and b-wave amplitudes that were not different from those in sham mice. This improvement in visual function also was associated with a significant reduction in retinal GFAP, neuroinflammation markers, and oxidative stress compared to saline-treated rOBI mice. *In vitro*, Müller cells exposed to oxidative stress via increasing doses of hydrogen peroxide demonstrated decreased viability, increased GFAP mRNA expression, and reduced activity for the antioxidant catalase. On the other hand, oxidatively stressed Müller cells pre-incubated with ASC-CCM showed normalized GFAP, viability, and catalase activity. In conclusion, our study demonstrates that a single intravitreal injection of ASC-CCM in the rOBI can significantly rescue retinal injury and provide significant restoration of visual function. Our *in vitro* studies suggest that the antioxidant catalase may play a major role in the protective effects of ASC-CCM, uncovering yet another aspect of the multifaceted benefits of ASC secretome therapies in neurotrauma.

Keywords

Explosive blast; Neurodegeneration; Müller; Inflammation; Retina; Confocal; Catalase

1. Introduction

Visual deficits are a common concern among subjects with head trauma yielding traumatic brain injury (TBI) (Sen, 2017). While brain injuries resulting from blast, impact, or the rapid acceleration and deceleration of the brain within the skull stemming from the bodily displacement caused by the blast, and associated visual deficits have been extensively reported (Dutca et al., 2014; Guley et al., 2016; Harper et al., 2019; Mammadova et al., 2017), direct primary ocular blast injuries i.e. those arising as a consequence of exposure of the eye to the blast wave alone (Allen et al., 2018; Bricker-Anthony et al., 2016; Vest et al., 2019) and their associated molecular mechanisms leading to retinal neurodegeneration have only recently been gaining attention (Rasiah et al., 2021). Blast injury caused by explosive munitions resulting in loss of vision is most prevalent in war-related injuries, with about 78.1% of total injuries worldwide representing ocular blast injuries (McMaster and Clare, 2020). Additionally, ocular injuries have been reported in fire and explosions in the civilian population, with a frequency of 2.13–28% in mass-casualty incidents (Carley and Mackway-Jones, 1997; Jiang et al., 2019; Liu et al., 2020; Odhiambo et al., 2002; Prevention, 2001; Yonekawa et al., 2014). Although open-globe injuries caused by the blast are readily diagnosed and the course of treatment clearcut, closed-globe injury from a blast wave is harder to recognize immediately following the blast, and therefore possibly overlooked for treatment in the field, often resulting in devastating disabilities that could potentially be prevented. An ocular blast itself can result in immediate retinal disruption and cell death; however, the surviving cells continue to experience the ripple effects of self-propagating cellular damage arising from increased cellular oxidative stress (among other possible phenomena), which can considerably worsen the outcome (Nidhi et al., 2018). Additionally, repetitive TBI or exposure to repeated blast injuries results in additive

or synergistic influences that are likely to further worsen the immediate outcome and the long-term worsening (Bailes et al., 2014; Engel et al., 2019).

Although many approaches have been tested in animal models and human clinical trials (Rasiah et al., 2021; Xiong et al., 2013), effective therapies for mitigating neurotrauma effects have not been developed. Stem cell therapies have gained recent attention in treating TBI and the associated visual deficits, some of which arise from indirect ocular injury from head trauma (Das et al., 2019a, 2019b). Much of our research has focused on therapeutic applications of adult mesenchymal stem cells (MSC) derived from the stromal fraction of human adipose tissue (ASC, adipose-derived stem/stromal cells) to accelerate the development of regenerative and neuroprotective therapies that treat retinal neuro-vascular pathology. Our recent work in a focal cranial blast model of TBI that results in indirect ocular injury has demonstrated that ASC concentrated conditioned medium (ASC-CCM), when delivered via the intravitreal route, yielded a significant restoration in vision accompanied by a decrease in retinal neuroinflammation in blast-injured TBI mice (Jha et al., 2018, 2019, 2021). The purpose of the current study is to extend our previous work to a closed-globe repetitive direct ocular blast model of retinal trauma to establish the preclinical efficacy of ASC-CCM. Identification of the molecular processes exacerbating retinal injury, such as increased cellular oxidative stress and neuroinflammation, in repetitive blast-associated neurotrauma can uncover specific pathogenic mechanisms to target for treatment and provide a platform for efficient testing of targeted stem cell-based therapeutics. We hypothesized that ASC-CCM delivered via the intravitreal route in a repetitive ocular blast injury model (rOBI) would decrease neuroinflammation and cellular oxidative stress in retina and restore vision following blast. We have found that a single intravitreal delivery of ASC-CCM decreased the levels of neuroinflammatory markers, reduced retinal injury as evidenced by normalized GFAP in Müller cells, decreased oxidative stress as evidenced by reduced DNA/RNA damage marker immunolabeling in the rOBI model, while also restoring b-wave amplitudes and visual acuity. In addition, using Müller cells *in vitro*, we demonstrate that the protective effects of ASC-CCM may be mediated (at least in part) via the antioxidant, catalase, uncovering yet another aspect of the multifaceted benefits of MSC secretome therapies in neurotrauma.

2. Methods

2.1. Animal care and procedures

Male 12-week old C57BL/6J mice were procured from The Jackson Laboratory (Bar Harbor, ME) and kept under 12 h light/12 h dark cycle at a temperature between 21 °C and 23 °C and allowed free access to food and water. Animal procedures were performed with the approval of the Institutional Animal Care and Use Committee, UTHSC, Memphis, and USAMRMC Animal Care and Use Review Office, and followed the guidelines of the Association for Research in Vision and Ophthalmology Statement on the Use of Animals in Ophthalmic and Vision Research and the guidelines of the Association for Assessment and Accreditation of Laboratory Animal Care. About 24 h before blast injury, animals received 32 mg/ml Acetaminophen (Infant's Tylenol, Cherry flavor, Walgreens Pharmacy)

provided in their drinking water, yielding a dose of 300 mg/kg/day. This continued until 72 h post-blast injury when normal water was provided.

Mice were anesthetized subcutaneously with ketamine (50 mg/kg) and dexmedetomidine (0.25 mg/kg) cocktail. Repetitive ocular blast injury model (rOBI) was performed as described previously (Bernardo-Colón et al., 2019; Hines-Beard et al., 2012; Vest et al., 2019), except that mouse received five repetitive ocular blasts (25 psi) with a 1-min interval between the blasts (Fig. 1A). The blast device that was used to produce a primary blast to the mouse eye was the same as previously described for use in the focal cranial blast (Guley et al., 2016, 2019; Honig et al., 2019), with a slight modification to the mouse holder only to expose the left eye. In brief, the anesthetized mice were secured to a cushioned sling, and the sling was inserted into polyvinyl chloride (PVC) pipe (25 mm inner diameter, 33 mm outer diameter), with the left side of the mouse head apposed to an 11 mm opening in the midpoint of one wall of the tube. This “inner” tube was slid into a 42 mm outer-diameter wide clear PVC pipe (34 mm inner diameter) with a 6.0 mm hole bored into the midpoint of its wall. The inner PVC tube was rotated in the outer PVC tube so that the left eye was positioned in the center of the 6.0 mm hole in the outer tube. The outer tube was mounted perpendicular to the blast cannon using two Plexiglas holders mounted on an x-y table, as described previously (Guley et al., 2016). The outer tube opening was then aligned with the gun barrel opening, using the x-y controls, so the mouse eye was about 8 mm from the blast cannon barrel tip. Thus, only the left eye was exposed to blast, and the rest of the body was shielded from the blast, as well as cushioned in the sling to minimize blast-induced movement (Guley et al., 2016). Mice that received a sham (0-psi) blast were handled in an identical way, but with a metal plate inserted between the barrel of the paintball gun and the mouse holder. About 2–3 h post-blast, rOBI animals either received an intravitreal injection of ASC-CCM (2μl/eye, ~200 ng of protein; rOBI-ASC-CCM) into both eyes or an equal volume of saline (rOBI-Sal). Animals that underwent a similar procedure excepting the blast exposure served as sham controls and received an equal volume of saline in both eyes (Sham-Sal). Animal anesthesia was reversed using Atipamezole Hydrochloride (0.25 mg/kg). Pilot studies that had been conducted with a lower dose of ASC-CCM than used here (1μl/eye, ~100 ng of protein) resulted in the minimal rescue of visual deficits (data not shown). Therefore, a higher dose was used as reported in this study. The rOBI of five repetitive blasts at 25-psi pressure with an interval of 1 min between blasts followed by intravitreal injection of either saline or ASC-CCM was well tolerated throughout the experimental period of 4 weeks. The retinal health was monitored by OCT imaging at 2 weeks after injury and treatment, with no major anomalies noted across groups (Supplemental Fig. 1). One animal in the rOBI group, however, developed a corneal haze and could not be imaged by OCT, and therefore was excluded from the analysis.

2.2. Electroretinography

To assess retinal function four weeks post rOBI, mice underwent ERG recording as described by us previously (Jha et al., 2019). Briefly, mice were dark-adapted overnight and were anesthetized with ketamine and dexmedetomidine. Corneas were topically anesthetized with proparacaine hydrochloride ophthalmic solution (Bausch & Lomb), and dilation was achieved with tropicamide ophthalmic solution (Bausch & Lomb). Retinal responses were

measured by electrodes placed on the corneal surface of each eye using the Celeris Electrodiagnostics (Diagnosys LLC) device and Touch/Touch protocol with the opposite eye serving as a reference. ERG stimuli consisted of three steps of Ganzfeld (0.01–1 cd $s.m^2$). Amplitudes were recorded for both a-wave and b-wave.

2.3. Optokinetic measurements

To assess retinal function four weeks post rOBI, visual acuity and contrast sensitivity were tested using an optokinetic device (OptoMotry unit; Cerebral Mechanics Inc., Alberta, Canada), as described by us previously (Jha et al., 2019). Visual acuity was assessed at 100% contrast by varying the spatial frequency. Contrast sensitivity was assessed in mice by varying the contrast at 0.042 cycles per degree (c/d) of spatial frequency.

2.4. Immunohistology and imaging

Four weeks post rOBI, animals were euthanized, eyes were enucleated and fixed with 4% paraformaldehyde in 0.1 phosphate buffer overnight at 4 °C. Eyes were then cryopreserved with 10–30% sucrose, embedded in optimal cutting temperature (OCT) embedding media (Tissue-Tek, Torrance, CA, USA), cut into 12 μm thick sections using a Microm™ HM550 Cryostat (GMI, Ramsey, MN, USA), and collected on Superfrost®/Plus microscope slides, as we previously described (Jha et al., 2018, 2021). Air-dried cryosections were briefly washed with PBS and blocked with 5% immunoglobulin-free BSA and 5% filtered goat serum in 0.3% Triton X-100 containing PBS for 30 min. Tissue sections were incubated overnight at 4 °C with the following primary antibodies: anti-nitrotyrosine antibody [HM.11] (Abcam, ab7048); Anti-DNA/RNA Damage antibody [15A3] (Abcam, ab62623); or anti-glial fibrillary acidic protein antibody (CiteAb, Z0334). Sections were washed and incubated with the appropriate Alexa Fluor (488 or 594) conjugated secondary antibodies (Invitrogen, Grand Island, NY, USA; at a 1: 200 dilution). Immunostained sections were photographed using a Zeiss LSM 710 laser scanning confocal microscope. Z-stack images were captured, followed by post-processing as maximum intensity projections. The resulting total pixel intensities in the regions of interest were quantified by ImageJ software. The relative fluorescence was expressed as mean intensity per 100,000 μm^2 of the retina.

2.5. rMC-1 cell culture and WST-1 assay

Immortalized retinal Müller cell line rMC-1 (Cat#ENW001, Kerafast) were maintained in Dulbecco's Modified Eagle Medium (DMEM) containing L-glutamine and supplemented with 10% of HI-FBS, 100 U/mL penicillin, and 100 μg/mL streptomycin in a humidified 5% CO_2 incubator at 37 °C. About 1×10^4 cells were pre-incubated with ~2 μg of ASC-CCM for ~6 h, and then exposed to increasing doses (0, 100, 200, and 400 μM) of H_2O_2 for 24 h in serum-free media. Cell viability was assessed using WST-1 Cell Proliferation Assay System (Takara Bio Inc; Cat #MK400) according to the manufacturer's protocol.

2.6. Oxidative stress/catalase activity assay

About 1×10^5 rMC-1 cells were pre-incubated with ~2 μg of ASC-CCM for ~6 h. To inhibit catalase activity, 3-Amino-1,2,4-triazole (3-AT), a known inhibitor of catalase, was used at 0.5 mM concentration 2 h before the addition of ASC-CCM. After 6 h, cells were exposed

to 200 μM of H_2O_2 for 4 h in serum-free media. At the conclusion of the study, cell lysates were harvested with RIPA buffer, and we proceeded with a catalase enzymatic activity assay, using the Colorimetric Activity Kit (Arbor Assays, Ann Arbor, MI. Cat# K033–H1) following the manufacturer's instructions.

2.7. Gene expression analysis

Total RNA was isolated from individual retinas and from *in vitro* cultured cells using NucleoSpin® RNA Plus kit (Macherey-Nagel GmbH) as per the manufacturer's protocol. After reverse transcription with the High-Capacity cDNA Reverse Transcription Kit (Applied Biosystems), cDNA was used for qPCR with Taqman probes (Table 1). The mRNA expression was normalized to the expression of 18s rRNA as the internal control as described by us previously (Jha et al., 2021).

2.8. Statistical analysis

Results are presented as mean ± standard error of the mean (SEM) for each group and groups compared to one another for the *in vivo* studies. *In vitro* experiments were performed in duplicates and repeated two-three times independently. A one-way parametric analysis of variance, followed by a post hoc Bonferroni test, was performed to evaluate the data for statistical significance, followed by a Student *t*-test for individual group comparisons. Analyses were carried out using SPSS 17 (IBM Inc., USA) or GraphPad Prism 6.0. A *p*-value less than 0.05 was considered significant.

3. Results

3.1. ASC-CCM ameliorates decreased visual acuity and increased contrast sensitivity in repetitive ocular blast injury (rOBI) mice

To better understand the therapeutic efficacy of ASC-CCM in direct ocular blast-induced visual deficits, optokinetic measurements were performed 4 weeks after treatment in all groups. Visual acuity (spatial frequency threshold) at high contrast (100% contrast) and contrast sensitivity thresholds at a low spatial frequency [0.042 cycles per degree (c/d), i.e., wide stripes] were measured (Fig. 1B). The visual acuity in rOBI mice that received saline was significantly decreased when compared with age-matched sham mice receiving saline in the blast eye (rOBI-Sal, 0.286 ± 0.004 c/d; Sham-Sal, 0.400 ± 0.002 c/d, $p < 0.001$). Remarkably, rOBI mice that received ASC-CCM demonstrated significantly greater acuity in the blast eye than in rOBI-Sal mice (rOBI-ASC-CCM, 0.338 ± 0.005 c/d, $p < 0.001$), but nonetheless still less than in sham. As in the case of visual acuity, rOBI mice showed a contrast sensitivity deficit, in this case, an increase in the contrast needed to detect 0.042 c/d in the blast eye (rOBI-Sal, 98.45% ± 0.469; Sham-Sal, 7.45% ± 1.36, $p < 0.001$) (i.e. an increased threshold), but the deficit was significantly lessened in rOBI mice receiving ASC-CCM (rOBI-ASC-CCM, 80.40% ± 1.86, $p < 0.001$), although a substantial deficit compared to sham remained.

3.2. ASC-CCM ameliorates decreased b-wave and a-wave amplitudes in rOBI mice

Dark-adapted scotopic ERG responses were recorded from the left eyes of mice in all experimental groups 4 weeks post injury and treatments. With increasing light intensities,

the expected increase in b-wave amplitudes could be discerned in all groups, but with a significant reduction noted in the rOBI mice as compared to sham mice across all light intensities (Fig. 2A). While the b-wave amplitude measured at 1 cd s.m^2 light intensity in the Sham-Sal group of animals was 498.8 ± 13.69 μV, in rOBI mice that received saline, it was significantly decreased to 420.04 ± 12.39 μV ($p < 0.001$). On the other hand, intravitreal injection of ASC-CCM resulted in significant improvement in the b-wave amplitude compared to the rOBI mice at 1 cd s.m^2 (rOBI-ASC-CCM, 459.31 ± 11.94 μV; $p < 0.05$). Similar to the b-wave, the a-wave amplitudes were decreased for rOBI-Sal mice, though only at the two higher light intensities. In particular, while the mean a-wave amplitude at 1 cd s.m^2 intensity in Sham-Sal group of animals was −270.58 ± 8.33 μV, it was significantly decreased to −234.4 ± 6.15 μV in rOBI mice that received saline ($p < 0.001$, Fig. 2B). By contrast, intravitreal injection of ASC-CCM resulted in restoration in the a-wave amplitude, reaching significance at 1 cd s.m2, when compared to rOBI mice that received saline (rOBI-ASC-CCM, −262.5 ± 7.9 μV; $p < 0.01$).

3.3. ASC-CCM ameliorates increased glial fibrillary acidic protein (GFAP) in rOBI mice correlated with Müller cells in vitro

GFAP immunoreactivity in Müller glial cells serves as a tool to assess retinal injury (Grosche et al., 1995; Jha et al., 2019). We determined whether rOBI itself increases GFAP in Müller cells, and whether treatment with ASC-CCM in mice subjected to rOBI attenuated any such Müller glial cell activation (Fig. 3). In the sham group, expression of GFAP was only observed in the nerve fiber layer, NFL (Fig. 3A), while in the rOBI group treated with saline, GFAP expression was observed in Müller glial processes that extended into the inner retina through the inner plexiform layer, IPL (Fig. 3B). In contrast, the rOBI group that received ASC-CCM demonstrated lower levels of GFAP immunolabeling than rOBI-Sal mice (Fig. 3C). The mean total pixel intensity of GFAP expression measured from NFL to the retinal pigment epithelium in the normal Sham-Sal group retina was 10.1 ± 2.9, while in the rOBI-Sal group, it was increased to 22.65 ± 5.22 (mean intensity/100,000 μm^2 area; $p < 0.01$, Fig. 3D). On the other hand, the rOBI-ASC-CCM group showed reduced GFAP expression compared to rOBI-Sal mice (14.58 ± 2.85 mean intensity/100,000 μm^2 area; $p < 0.01$). The increased GFAP immunoreactivity in the rOBI-Sal mice was confirmed at the mRNA level by a >2-fold retinal increase in the rOBI-Sal group (2.33 ± 0.46, $p < 0.003$) compared to Sham-Sal group retina, as detected by qPCR. Similarly, the rOBI group that received ASC-CCM demonstrated significantly lower levels of retinal GFAP mRNA (0.82 ± 0.09, $p < 0.003$; Fig. 3E) than rOBI-Sal mice. Interestingly, increased GFAP expression *in vivo* following rOBI could be demonstrated *in vitro* using rat rMC-1 Müller glial cells challenged with oxidative stress (Fig. 3F). With an increasing dose of hydrogen peroxide (H_20_2) to produce the stress, a 1.5–2.0-fold increase in GFAP mRNA expression was noted. On the other hand, those cells challenged with H_20_2 but pre-incubated with ASC-CCM exhibited GFAP mRNA expression levels similar to non-challenged cells ($p < 0.001$; Fig. 3G).

3.4. ASC-CCM ameliorates increased neuroinflammation markers in rOBI mice

Previous studies using a focal cranial blast model of TBI (Guley et al., 2019; Honig et al., 2019; Jha et al., 2018, 2019) or ocular blast trauma (Bernardo-Colón et al., 2018)

have demonstrated increased inflammation in the visual system associated with loss of visual function. Therefore, to further examine the inflammatory response in this model of primary blast exposure to the eye, we assayed inflammatory cytokine levels in the whole retina following rOBI. We examined the mRNA expression of pro-inflammatory cytokines and cell adhesion molecules, namely, TNF-α, ICAM1, and CCL2, along with markers for microglia/macrophage activation (IL-1β and CD86) 4 weeks post injury and treatment in all groups (Fig. 4). Retinal extracts from rOBI mice receiving saline showed increased levels of TNF-α (2.24 ± 0.34, $p < 0.003$); CCL2 (2.27 ± 0.20, $p < 0.001$); and ICAM1 (1.40 ± 0.13, $p < 0.06$) compared to sham, with a significant reduction for these in rOBI mice receiving ASC-CCM [TNF-α (0.64 ± 0.16, $p < 0.003$); CCL2 (0.88 ± 0.16, $p < 0.001$); ICAM1 (0.80 ± 0.11, $p < 0.06$)] compared to rOBI-Sal mice, suggesting that ASC-CCM attenuates pro-inflammatory gene expression after rOBI. In accordance with our previous observation that microglial activation/polarization towards the M1 phenotype as evidenced by increased expression of CD86 and IL-1β occurs in TBI retina (Jha et al., 2018), rOBI mice demonstrated a significant increase in IL-1β (1.57 ± 0.16, $p < 0.02$) and CD86 (1.88 ± 0.36, $p < 0.04$) gene transcripts compared to Sham-Sal mice, with a significant reduction in rOBI mice receiving ASC-CCM [IL-1β (0.80 ± 0.09, $p < 0.02$) and CD86 (0.62 ± 0.09, $p < 0.04$)] compared to rOBI-Sal mice.

3.5. ASC-CCM ameliorates increased oxidative stress in rOBI mice

Because oxidative DNA/RNA damage and protein nitration can lead to defects in gene expression and protein synthesis (Honda et al., 2005), with important implications in neurodegenerative disorders (Nunomura et al., 2006), we assessed if rOBI mice show increased retinal oxidative stress. The occurrence of oxidative base modification to DNA and RNA in the retina was evaluated by an antibody that detects oxidized base modification in DNA: Oxo-8-dG (8-Oxo-7,8-dihydro-2′-deoxyguanosine), and 8-hydroxyguanine, (7,8-Dihydro-8-oxoguanine), and in RNA: Oxo-8-G (8-oxo-7,8-dihydroguanosine); while protein nitration was evaluated by an antibody against nitrotyrosine in the retina. Whereas Sham-Sal retina showed minimal immunostaining with the DNA/RNA damage marker antibody (Fig. 5A), increased immunostaining was observed in rOBI mice receiving saline in the ganglion cell layer, (GCL), as well as in the inner nuclear layer (INL) (Fig. 5B). Interestingly, intravitreal treatment with ASC-CCM in rOBI mice demonstrated decreased labeling of the DNA/RNA damage marker immunostaining compared to saline-injected rOBI mice (Fig. 5C, Supplemental Fig. 2). The mean total pixel intensity of the immunolabeling for the DNA/RNA damage marker measured from NFL to retinal pigment epithelium in the normal Sham-Sal group retina was 3.97 ± 1.09, while in the rOBI group with saline, it was 16.68 ± 5.36 (mean intensity/100, 000 μm^2 area; $p < 0.001$, Fig. 5D). On the other hand, rOBI mice with ASC-CCM showed reduced DNA/RNA marker immunolabeling compared to saline-injected rOBI mice (6.26 ± 1.28 mean intensity/100, 000 μm^2 area; $p < 0.001$).

The retinal stress stemming from nitric oxide (NO)-mediated nitrosylation of redox-sensitive proteins was analyzed using an antibody to nitrotyrosine. While the Sham-Sal mice retinas showed minimal immunostaining for the anti-nitrotyrosine antibody (Fig. 5E), increased immunostaining was observed in the cytoplasm of ganglion cells of rOBI mice receiving saline (Fig. 5F). Retinal sections incubated without the primary antibody revealed the

specificity of immunostaining (Supplemental Fig. 3). Interestingly, intravitreal treatment with ASC-CCM in rOBI mice yielded decreased expression of immunostaining compared to rOBI-Sal mice, suggesting a decreased nitrosative stress (Fig. 5G). The mean total pixel intensity of anti-nitrotyrosine measured from NFL to the retinal pigment epithelium in normal Sham-Sal group retinas was 24.67 ± 1.17 while for the rOBI group treated with saline, it was 46.81 ± 3.11 (mean intensity/100,000 μm^2 area; $p < 0.001$, Fig. 5H). On the other hand, rOBI mice treated with ASC-CCM showed reduced anti-nitrotyrosine levels compared to rOBI-Sal mice (20.92 ± 2.3 mean intensity/100,000 μm^2 area; $p < 0.001$). Taken together with the results for the DNA/RNA damage marker, the reduction in anti-nitrotyrosine signal supports the claim that ASC-CCM treatment ameliorates increased oxidative stress in rOBI mice.

3.6. ASC-CCM ameliorates increased oxidative stress and decreased activity of the antioxidant catalase in Müller cells in vitro

To evaluate the beneficial antioxidant influence of ASC-CCM on Müller cells, we next assessed H_2O_2-induced damage in Müller cells with and without ASC-CCM *in vitro*. To this end, first, we assessed the viability of rMC-1 cells exposed to H_2O_2 in the presence or absence of ASC-CCM. As expected, with increasing doses of H_2O_2, a decrease in the cleavage of the tetrazolium salt to formazan by cellular mitochondrial dehydrogenase was observed (indicative of decreased viability), with the highest H_2O_2 dose showing the most significant decrease in cell viability. On the other hand, rMC-1 cells that were pre-incubated with ASC-CCM and challenged with H_2O_2 demonstrated better cell viability at 100 and 200 μM but not 400 μM H_2O_2 than those not pre-incubated with ASC-CCM (Fig. 5I & Supplemental Fig. 4). Previously we have shown that ASC-CCM contains abundant levels of antioxidant proteins such as IDO-1 and SOD2/3 (Jha et al., 2018). Since catalase (another antioxidant enzyme) is prominently involved in the breakdown of H_2O_2 into the water and molecular oxygen, thus curtailing oxidative damage and is also known to be found in the secreted extracellular vesicles (EVs) of mesenchymal stem cells (MSCs) such as our ASC (Bodart-Santos et al., 2019), we assessed the catalase activity in our rMC-1 cells exposed to H_2O_2 with and without ASC-CCM (Fig. 5K). While untreated control rMC-1 cells had 51.4 ± 0.5 U of catalase activity in the cell lysates, cells exposed to a 200 μM H_2O_2 demonstrated 43.0 ± 0.7 U, a significant reduction in catalase activity compared to untreated cells ($p < 0.001$; Fig. 5K). Thus, oxidative stress via H_2O_2 appears to reduce catalase activity and thereby potentially worsen oxidative stress. On the other hand, cells pre-incubated with ASC-CCM and exposed to H_2O_2 demonstrated 49.5 ± 1.2 U, significantly greater ($p < 0.001$; Fig. 5K) catalase activity than cells exposed to H_2O_2 without ASC-CCM, and were not different from control cells. Finally, preincubation of ASC-CCM with the catalase inhibitor 3-AT reduced catalase activity in the cell lysates to 41.3 ± 0.3 U, which did not differ from that in cells untreated with ASC-CCM and exposed to H_2O_2 ($p > 0.05$; Fig. 5K).

4. Discussion

This study indicates that repetitive ocular blast can result in retinal injury and severe impairment in visual function. Our studies suggest that increased oxidative stress and ongoing neuroinflammation may likely worsen the injury processes and the outcome after

ocular trauma. Interestingly, we found that a single intravitreal injection of ASC-CCM significantly reduces signs of oxidative and neuroinflammatory injury processes, and reduces the retinal injury and dysfunction associated with repeat ocular blast injury. In addition, using Müller cells *in vitro*, we demonstrate that the protective effects of ASC-CCM are potentially associated with a particular role of the antioxidant catalase. Our previous studies have shown the preclinical efficacy of ASC-CCM in ameliorating the visual deficits after a focal cranial blast that indirectly injures the retina (Jha et al., 2018, 2019, 2021), and our current results demonstrate the efficacy of ASC-CCM in the direct ocular blast model as well, suggesting that ASC-CCM is a potent neuroprotective agent against the adverse consequences of diverse types of ocular trauma.

Oxidative damage to nucleic acids is a common event observed in postmortem brains and serum of TBI subjects (Lorente et al., 2020). The association of DNA and RNA oxidative damage with mortality in TBI patients suggests a critical role of oxidative stress related damage in the pathophysiology of TBI (Lorente et al., 2020). Oxidative stress results in oxidative base modifications to both DNA and RNA, which can compromise neuronal function and cause progressive neurodegeneration (Nunomura et al., 2006). While Oxo-8-dG and 8-hydroxyguanine serve as excellent markers for DNA damage produced by oxidants, Oxo-8-G is associated with oxidative RNA damage that typically leads to defects in protein synthesis (Honda et al., 2005; Nunomura et al., 2006). Using a validated anti-DNA/RNA oxidative damage antibody, we show that rOBI results in extensive oxidative stress in the GCL that extends into the INL of the retina as compared to sham injury mice. Our functional data suggests that these oxidative changes are detrimental to ocular function. In support of an adverse effect of the oxidative base modification to DNA and RNA of cells in the GCL, such oxidative changes have also been shown in other OBI studies and other retinal neurodegenerative models, including the repeated ocular blast model (Bernardo-Colón et al., 2018), retinal I/R injury model (Chen and Tang, 2011), subretinal lipid induced age-related macular degeneration model (Kim et al., 2021), and light-induced damage models of injury (Giacci et al., 2014). Notably, retinal ganglion cell injury in the ocular blast model is indicated by optic nerve axon loss (Bernardo-Colón et al., 2018). Interestingly, immunolabeling experiments in the light-induced damage model demonstrated Oxo-8-dG immunostaining is predominately associated with GFAP positive Müller cells (Giacci et al., 2014), suggesting Müller cells are important target cells of the oxidative nucleic acid injury. Since the immunolabeling of Oxo-8-dG in our studies demonstrated prominent cytoplasmic staining, it is possible that the DNA damage was associated with mitochondrial DNA. The increased accumulation of Oxo-8-dG in mitochondrial DNA needs further exploration, as the mitochondrion is both a major source of reactive oxygen species (ROS) production and a primary target of oxidative damage in the cell (Murphy, 2009). While the specific mechanism through which increased DNA/RNA damage occurs in rOBI mice is unknown, a single intravitreal delivery of ASC-CCM significantly prevented such an increase in DNA/RNA damage, however, it is not completely mitigated. Recently, MSCs have been shown to transfer mitochondria to target tissues through a phenomenon known as mitoception to impart their benefits (Court et al., 2020). Whether such a mechanism may be operative in their benefit in rOBI needs further exploration.

Nitrotyrosine represents an additional marker of oxidative stress, in this case, associated with protein dysfunction, that is increased in the retina of rOBI mice, with a significant reversal to sham levels in rOBI mice receiving ASC-CCM. Chemical oxidation of tyrosine with peroxynitrite ($ONOO^-$) or via the enzymatic action of peroxidases with nitrite and hydrogen peroxide leads to the generation of nitrotyrosine (Pacher et al., 2007). A variety of animal models of neurodegenerative diseases, including a subretinal lipid-induced age-related macular degeneration model (Kim et al., 2021), diabetic retinopathy (Abouhish et al., 2020), fetal hypoxia-reoxygenation injury (Vasquez-Vivar et al., 2020), and retinal I/R injury models (Shimouchi et al., 2016), have shown similarly increased nitrotyrosine. Increased nitrotyrosine levels have also been shown to be correlated with dysfunctional proteins, specifically with antioxidant enzymes such as catalase, suggesting amplified oxidative stress and inflammatory milieu under such conditions (Ghosh et al., 2006).

The retina contains a variety of oxidative stress defense mechanisms, of which antioxidant enzymes such as superoxide dismutase, glutathione peroxidase (GPx) and, catalase are known to play a vital role (Álvarez-Barrios et al., 2021). Catalase and GPx are key enzymatic catalysts involved in the conversion of highly reactive H_2O_2, either via decomposition to water and O_2 by catalase, often associated with peroxisomal compartment, or via oxidation of GSH by GPx, using H_2O_2, to form the disulfide GSSH and water (Chen et al., 2009). In the retina, catalase is highly expressed in the photoreceptor inner segments and retinal pigment epithelium (Atalla et al., 1987), whose augmentation by gene therapy or cell-penetrating catalase derivatives has been shown to be protective against the retinal oxidative stress (Giordano et al., 2015; Rex et al., 2004). Interestingly, Müller cells exposed to H_2O_2 in our study demonstrated a significant reduction in catalase activity. It is not known if this reduction in catalase activity is due to altered catalase gene expression and/or degradation of the enzyme. Although the potential mechanism underlying the reduction in catalase activity is unclear, the reduction is likely to be harmful, given that other studies have shown that reduction in catalase activity make cells susceptible for oxidative stress (Scott et al., 1993). Recently, EVs derived from MSCs were found to transfer active catalase enzyme into hippocampal neurons to protect them from oxidative stress induced by soluble oligomers of the amyloid-β peptide (Bodart-Santos et al., 2019). Since ASC-CCM comprises EVs, it is possible that such a transfer of catalase from the ASC-CCM may be operative in the retinal rescue by ASC-CCM, particularly for Müller cells, as shown by our *in vitro* studies. Our pilot proteomic analysis indeed confirmed the presence of catalase in the EVs in MSC (data not shown). It is conceivable that EVs isolated by the standard procedures of ultracentrifugation (Potter et al., 2018) or a commercial size-exclusion column-based EV purification method (Liangsupree et al., 2021) could be used to isolate such EVs from ASC-CCM to test the hypothesis that EV-derived catalase in ASC-CCM indeed serves to transfer active catalase enzyme to Müller cells *in vitro*. In support of our hypothesis, studies using 3-AT, a known catalase inhibitor, suggests that catalase activity in ASC-CCM is potentially involved in the rescue effect observed in Müller cells *in vitro*. In line with our data, a recent clinical study conducted in the minimally conscious subjects treated with bone marrow-derived MSC suggests that MSCs modulate oxidative stress via catalase activity (Jezierska-Wozniak et al., 2020).

Increased oxidative stress and increased inflammation reflected in the upregulation of pro-inflammatory cytokines have been reported in the retina following ocular blast trauma, but it is uncertain if oxidative stress causes inflammation or vice versa (Bernardo-Colón et al., 2018). Similarly, we found upregulation in the retina of pro-inflammatory (TNF-α, CCL2, and ICAM-1) and microglia/macrophage (CD86 and IL-1β) gene transcripts in rOBI mice. Note that oxidative stress has been suggested to be a driver of neuroinflammation by other investigators (He et al., 2021), and so it could be the case that the increased retinal oxidative stress seen in our rOBI-Sal mice could have been the driver of the neuroinflammation marker increases we saw by qPCR. Interestingly, this increase in pro-inflammatory cytokines occurred in conjunction with increased GFAP mRNA and protein in the rOBI mice, suggesting retinal injury by either or both oxidative stress and neuroinflammation. This increase in GFAP in rOBI mice could be mimicked *in vitro* in rMC-1 cells acutely exposed to H_2O_2-mediated oxidative stress. However, it must be stressed that the artificially high levels of H_2O_2 exposure *in vitro* likely provide a different signaling environment to that in the neural retina after blast exposure. Previously we have shown that rMC-1 Müller cells *in vitro* respond to exogenous glutamate by altering their expression of GFAP with a compensatory decrease in glutamine synthetase and glutamate transporter (GLAST), suggesting that the rMC-1 cell line is a suitable line to test the biopotency of therapeutics (Jha et al., 2021). In this regard, we show that pretreatment of rMC-1 cells with ASC-CCM alleviated H_2O_2-induced increases in GFAP and improved their cell viability. Although this beneficial effect of ASC-CCM *in vitro* in isolated Müller cells is intriguing, it is unclear if Müller cells are the target of ASC-CCM *in vivo*. Therefore, future studies deciphering the cellular targets of ASC-CCM and/or the components of ASC-CCM are necessary to establish the basis of the therapeutic effects of ASC-CCM in rOBI mice.

One compelling feature of our study is that intravitreal delivery of ASC-CCM into the rOBI mice resulted in the significant rescue of visual function. Optokinetic measurements performed 4-weeks post-rOBI in saline-injected mice revealed a significant decrease in the visual acuity in the injured eye and a comparable increase in the contrast sensitivity threshold (meaning reduced contrast sensitivity). Intravitreal delivery of ASC-CCM into the injured eye significantly rescued the visual acuity and contrast sensitivity deficits. A similar pattern of the deficit with rOBI and rescue with ASC-CCM was seen for the scotopic ERG b-wave amplitudes (predominantly elicited from bipolar and Müller cells) and a-wave-amplitudes (elicited from rod photoreceptors), further confirming retinal injury with rOBI and a neuroprotective effect of ASC-CCM in the rOBI mice. It is worth noting that while b-wave amplitudes were lower in rOBI mice than sham-treated eyes at all three light intensities, the amplitude of the a-wave post-rOBI was significantly different from that of sham-treated eyes only at 1 cd s.m^2. Interestingly, in those rOBI mice receiving ASC-CCM, a-wave amplitudes were indistinguishable from those in sham mice and, more importantly, significantly improved at 1 cd s.m^2 compared to rOBI mice receiving saline.

We readily recognize some limitations of this study. Firstly, a possibility that ASC-CCM acts through an antioxidant defense mechanism and mainly via catalase activity is descriptive with no causal link established. Future studies are needed to either knock down catalase in Müller cells or overexpress catalase in MSCs to further establish the role of catalase in the observed benefits. Secondly, the rescue of visual function was incomplete in

the case of acuity and contrast sensitivity, being only 20–30% with ASC-CCM. This may be due to an inadequate amount of ASC-CCM proteins (2μl/eye, ~200 ng of protein) delivered, as 1μl/eye demonstrated even lesser recovery for contrast sensitivity (data not shown). This highlights the potential shortcomings of acute, single-dose, intravitreal therapy and suggests either repeated dosing or a sustained delivery mechanism would be beneficial. Thirdly, our studies in rOBI mice did not examine well-established other deficits or pathologies observed in rOBI models, including reduced visually evoked potentials or degenerative axons in the optic nerve (Bricker-Anthony et al., 2016; Vest et al., 2019) to discern the effects of ASC-CCM on other visual endpoints. Fourthly, traumatic ocular injuries can occur in low-resource settings where immediate intervention is inaccessible (e.g. war zones), resulting in worse cognitive and visual outcomes or increasing the time needed for rehabilitation. While immediate injection following blast exposure is modeled in the current study, we have not assessed the potential therapeutic window for ASC-CCM by evaluating later treatment time point(s) following blast exposure. To this end, the recent guidelines initiated by Brain Trauma Blueprint, recommends testing the optimal timing of a potential therapeutic be assessed prior to clinical translation (Smith et al., 2021). Fifthly, our studies in rOBI mice did not address the cellular and mechanistic source(s) of ROS in the retina after blast exposure. As part of normal physiology, the retina produces low levels of ROS that include H_2O_2 and superoxide radicals to support cellular adaptation to a changing environment and stress (Sies and Jones, 2020). However, when the redox system is off-balance, increased ROS accumulation occurs, which is strongly linked to neurodegeneration (Naguib et al., 2021). A number of possible mechanisms, including but not limited to mitochondrial dysfunction, increase in NADPH oxidase (NOX), and/or increased NOX enzyme activity, might be in play in the observed increase in ROS (Sies and Jones, 2020). Another alternate source of oxidative stress comes from excessive intracellular iron, which through a non-enzymatic Fenton or Haber-Weiss reaction (Mehlhase et al., 2006) can generate hydroxyl radicals, the most reactive form of ROS in TBI (Nisenbaum et al., 2013). Regardless of the source of ROS, it is interesting to note that intravitreal delivery of ASC-CCM significantly alleviated the increase in oxidative stress in rOBI mice. Finally, our studies did not attempt to study overt cell death in the retina following rOBI following the oxidative stress damage. Future studies using Caspase-1/3 or TUNEL staining might be useful to develop causal connection of increased oxidative stress to neurodegeneration in the model.

In conclusion, our study demonstrates that a single intravitreal injection of ASC-CCM following repetitive direct ocular blast can result in a significant rescue in retinal injury and significant restoration of visual function. Taken together with our previous studies involving mild TBI models, the current study establishes the value of a stem cell-based approach to treat neurotrauma. Future studies should incorporate this knowledge to develop effective regenerative therapies to restore visual system damage after TBI.

Supplementary Material

Refer to Web version on PubMed Central for supplementary material.

Acknowledgments

This study was funded by grants from the Department of Defense (W81XWH-16-1-0778), National Eye Institute (EY023427), and unrestricted funds from Research to Prevent Blindness to RG and Department of Defense (W81XWH-16-1-0076) to AR. KAJ and PR are the recipients of a postdoc fellowship award from the Neuroscience Institute, UTHSC. The funders played no role in the conduct of the study, collection of data, management of the study, analysis of data, interpretation of data, or preparation of the manuscript.

Glossary

TBI	Traumatic brain injury
MSC	Mesenchymal stem cell
ASC-CCM	Adiposederived stem/stromal cell concentrated conditioned medium
rOBI	Repetitive ocular blast injury
ERG	Electroretinography
OKN	Optokinetic reflex nystagmus

References

Abouhish H, Thounaojam MC, Jadeja RN, Gutsaeva DR, Powell FL, Khriza M, Martin PM, Bartoli M, 2020. Inhibition of HDAC6 attenuates diabetes-induced retinal redox imbalance and microangiopathy. Antioxidants 9.

Allen RS, Motz CT, Feola A, Chesler KC, Haider R, Ramachandra Rao S, Skelton LA, Fliesler SJ, Pardue MT, 2018. Long-term functional and structural consequences of primary blast overpressure to the eye. J. Neurotrauma 35, 2104–2116. [PubMed: 29648979]

Álvarez-Barrios A, Álvarez L, García M, Artime E, Pereiro R, González-Iglesias H, 2021. Antioxidant Defenses in the Human Eye: A Focus on Metallothioneins. Antioxidants (Basel), vol. 10. mdpi, p. 89. [PubMed: 33440661]

Atalla L, Fernandez MA, Rao NA, 1987. Immunohistochemical localization of catalase in ocular tissue. Curr. Eye Res. 6, 1181–1187. [PubMed: 3500016]

Bailes JE, Dashnaw ML, Petraglia AL, Turner RC, 2014. Cumulative effects of repetitive mild traumatic brain injury. Prog. Neurol. Surg. 28, 50–62. [PubMed: 24923392]

Bernardo-Colón A, Vest V, Clark A, Cooper ML, Calkins DJ, Harrison FE, Rex TS, 2018. Antioxidants prevent inflammation and preserve the optic projection and visual function in experimental neurotrauma. Cell Death Dis. 9, 1097, 1097. [PubMed: 30367086]

Bernardo-Colón A, Vest V, Cooper ML, Naguib SA, Calkins DJ, Rex TS, 2019. Progression and pathology of traumatic optic neuropathy from repeated primary blast exposure. Front. Neurosci. 13, 719. [PubMed: 31354422]

Bodart-Santos V, de Carvalho LRP, de Godoy MA, Batista AF, Saraiva LM, Lima LG, Abreu CA, De Felice FG, Galina A, Mendez-Otero R, Ferreira ST, 2019. Extracellular vesicles derived from human Wharton's jelly mesenchymal stem cells protect hippocampal neurons from oxidative stress and synapse damage induced by amyloid-β oligomers. Stem Cell Res. Ther. 10, 332. [PubMed: 31747944]

Bricker-Anthony C, Hines-Beard J, Rex TS, 2016. Eye-directed overpressure airwave-induced trauma causes lasting damage to the anterior and posterior globe: a model for testing cell-based therapies. J. Ocul. Pharmacol. Therapeut. 32, 286–295.

Carley SD, Mackway-Jones K, 1997. The casualty profile from the Manchester bombing 1996: a proposal for the construction and dissemination of casualty profiles from major incidents. J. Accident Emergency Med. 14, 76–80.

Chen B, Tang L, 2011. Protective effects of catalase on retinal ischemia/reperfusion injury in rats. Exp. Eye Res. 93, 599–606. [PubMed: 21824472]

Chen Y, Mehta G, Vasiliou V, 2009. Antioxidant Defenses in the ocular surface. Ocul. Surf. 7, 176–185. [PubMed: 19948101]

Court AC, Le-Gatt A, Luz-Crawford P, Parra E, Aliaga-Tobar V, Bátiz LF, Contreras RA, Ortúzar MI, Kurte M, Elizondo-Vega R, Maracaja-Coutinho V, Pino-Lagos K, Figueroa FE, Khoury M, 2020. Mitochondrial transfer from MSCs to T cells induces Treg differentiation and restricts inflammatory response. EMBO Rep. 21, e48052. [PubMed: 31984629]

Das M, Mayilsamy K, Mohapatra SS, Mohapatra S, 2019a. Mesenchymal stem cell therapy for the treatment of traumatic brain injury: progress and prospects. Rev. Neurosci. 30, 839–855. [PubMed: 31203262]

Das M, Tang X, Mohapatra SS, Mohapatra S, 2019b. Vision impairment after traumatic brain injury: present knowledge and future directions. Rev. Neurosci. 30, 305–315. [PubMed: 30226209]

Dutca LM, Stasheff SF, Hedberg-Buenz A, Rudd DS, Batra N, Blodi FR, Yorek MS, Yin T, Shankar M, Herlein JA, Naidoo J, Morlock L, Williams N, Kardon RH, Anderson MG, Pieper AA, Harper MM, 2014. Early detection of subclinical visual damage after blast-mediated TBI enables prevention of chronic visual deficit by treatment with P7C3-S243. Invest. ophthalmol. visual sci. 55, 8330–8341. [PubMed: 25468886]

Engel CC, Hoch E, Simmons MM, 2019. The neurological effects of repeated exposure to military occupational blast: implications for prevention and health. In: Proceedings, Findings, and Expert Recommendations from the Seventh Department of Defense State-Of-The-Science Meeting. RAND Corporation, Santa Monica, CA.

Ghosh S, Janocha AJ, Aronica MA, Swaidani S, Comhair SAA, Xu W, Zheng L, Kaveti S, Kinter M, Hazen SL, Erzurum SC, 2006. Nitrotyrosine proteome survey in asthma identifies oxidative mechanism of catalase inactivation. J. Immunol. 176, 5587–5597. [PubMed: 16622028]

Giacci MK, Wheeler L, Lovett S, Dishington E, Majda B, Bartlett CA, Thornton E, Harford-Wright E, Leonard A, Vink R, Harvey AR, Provis J, Dunlop SA, Hart NS, Hodgetts S, Natoli R, Van Den Heuvel C, Fitzgerald M, 2014. Differential effects of 670 and 830 nm red near infrared irradiation therapy: a comparative study of optic nerve injury, retinal degeneration, traumatic brain and spinal cord injury. PLoS One 9, e104565 e104565. [PubMed: 25105800]

Giordano CR, Roberts R, Krentz KA, Bissig D, Talreja D, Kumar A, Terlecky SR, Berkowitz BA, 2015. Catalase therapy corrects oxidative stress-induced pathophysiology in incipient diabetic retinopathy. Invest. Ophthalmol. Vis. Sci. 56, 3095–3102. [PubMed: 25813998]

Grosche J, Hartig W, Reichenbach A, 1995. Expression of glial fibrillary acidic protein (GFAP), glutamine synthetase (GS), and Bcl-2 protooncogene protein by Muller (glial) cells in retinal light damage of rats. Neurosci. Lett. 185, 119–122. [PubMed: 7746501]

Guley NH, Rogers JT, Del Mar NA, Deng Y, Islam RM, D'Surney L, Ferrell J, Deng B, Hines-Beard J, Bu W, Ren H, Elberger AJ, Marchetta JG, Rex TS, Honig MG, Reiner A, 2016. A novel closed-head model of mild traumatic brain injury using focal primary overpressure blast to the cranium in mice. J. Neurotrauma 33, 403–422. [PubMed: 26414413]

Guley NM, Del Mar NA, Ragsdale T, Li C, Perry AM, Moore BM, Honig MG, Reiner A, 2019. Amelioration of visual deficits and visual system pathology after mild TBI with the cannabinoid type-2 receptor inverse agonist SMM-189. Exp. Eye Res. 182, 109–124. [PubMed: 30922891]

Harper MM, Woll AW, Evans LP, Delcau M, Akurathi A, Hedberg-Buenz A, Soukup DA, Boehme N, Hefti MM, Dutca LM, Anderson MG, Bassuk AG, 2019. Blast preconditioning protects retinal ganglion cells and reveals targets for prevention of neurodegeneration following blast-mediated traumatic brian injury. Invest. ophthalmol. visual sci. 60, 4159–4170. [PubMed: 31598627]

He J, Liu J, Huang Y, Tang X, Xiao H, Hu Z, 2021. Oxidative stress, inflammation, and autophagy: potential targets of mesenchymal stem cells-based therapies in ischemic stroke. Front. Neurosci. 15, 641157. [PubMed: 33716657]

Hines-Beard J, Marchetta J, Gordon S, Chaum E, Geisert EE, Rex TS, 2012. A mouse model of ocular blast injury that induces closed globe anterior and posterior pole damage. Exp. Eye Res. 99, 63–70. [PubMed: 22504073]

Honda K, Smith MA, Zhu X, Baus D, Merrick WC, Tartakoff AM, Hattier T, Harris PL, Siedlak SL, Fujioka H, Liu Q, Moreira PI, Miller FP, Nunomura A, Shimohama S, Perry G, 2005. Ribosomal RNA in Alzheimer disease is oxidized by bound redox-active iron. J. Biol. Chem. 280, 20978–20986. [PubMed: 15767256]

Honig MG, Del Mar NA, Henderson DL, Ragsdale TD, Doty JB, Driver JH, Li C, Fortugno AP, Mitchell WM, Perry AM, Moore BM, Reiner A, 2019. Amelioration of visual deficits and visual system pathology after mild TBI via the cannabinoid Type-2 receptor inverse agonism of raloxifene. Exp. Neurol. 322, 113063. [PubMed: 31518568]

Jezierska-Wozniak K, Sinderewicz E, Czelejewska W, Wojtacha P, Barczewska M, Maksymowicz W, 2020. Influence of bone marrow-derived mesenchymal stem cell therapy on oxidative stress intensity in minimally conscious state patients. J. Clin. Med. 9, 683. [PubMed: 32138308]

Jha KA, Gentry J, Del Mar NA, Reiner A, Sohl N, Gangaraju R, 2021. Adipose tissue-derived mesenchymal stem cell concentrated conditioned medium alters the expression pattern of glutamate regulatory proteins and aquaporin-4 in the retina after mild traumatic brain injury. J. Neurotrauma 38, 1702–1716. [PubMed: 33183134]

Jha KA, Pentecost M, Lenin R, Gentry J, Klaic L, Del Mar N, Reiner A, Yang CH, Pfeffer LM, Sohl N, Gangaraju R, 2019. TSG-6 in conditioned media from adipose mesenchymal stem cells protects against visual deficits in mild traumatic brain injury model through neurovascular modulation. Stem Cell Res. Ther. 10, 318. [PubMed: 31690344]

Jha KA, Pentecost M, Lenin R, Klaic L, Elshaer SL, Gentry J, Russell JM, Beland A, Reiner A, Jotterand V, Sohl N, Gangaraju R, 2018. Concentrated conditioned media from adipose tissue derived mesenchymal stem cells mitigates visual deficits and retinal inflammation following mild traumatic brain injury. Int. J. Mol. Sci. 19.

Jiang H, Xue C, Gao Y, Wang Y, 2019. Analysis of ocular injury characteristics in survivors of the 8.12 tianjin port explosion, China. J. ophthalmol. 1360805, 1360805.

Kim S-Y, Kambhampati SP, Bhutto IA, McLeod DS, Lutty GA, Kannan RM, 2021. Evolution of oxidative stress, inflammation and neovascularization in the choroid and retina in a subretinal lipid induced age-related macular degeneration model. Exp. Eye Res. 203, 108391. [PubMed: 33307075]

Liangsupree T, Multia E, Riekkola M-L, 2021. Modern isolation and separation techniques for extracellular vesicles. J. Chromatogr. A 1636, 461773. [PubMed: 33316564]

Liu Y, Feng K, Jiang H, Hu F, Gao J, Zhang W, Zhang W, Huang B, Brant R, Zhang C, Yan H, 2020. Characteristics and treatments of ocular blast injury in Tianjin explosion in China. BMC Ophthalmol. 20, 185. [PubMed: 32375694]

Lorente L, Martín MM, González-Rivero AF, Pérez-Cejas A, Abreu-González P, Ramos L, Argueso M, Cáceres JJ, Solé-Violán J, Alvarez-Castillo A, Jiménez A, García-Marín V, 2020. Association between DNA and RNA oxidative damage and mortality of patients with traumatic brain injury. Neurocritical Care 32, 790–795. [PubMed: 31385181]

Mammadova N, Ghaisas S, Zenitsky G, Sakaguchi DS, Kanthasamy AG, Greenlee JJ, West Greenlee MH, 2017. Lasting retinal injury in a mouse model of blast-induced trauma. Am. J. Pathol. 187, 1459–1472. [PubMed: 28606756]

McMaster D, Clare G, 2020. Incidence of ocular blast injuries in modern conflict. Eye.

Mehlhase J, Gieche J, Widmer R, Grune T, 2006. Ferritin levels in microglia depend upon activation: modulation by reactive oxygen species. Biochim. Biophys. Acta 1763, 854–859. [PubMed: 16777245]

Murphy MP, 2009. How mitochondria produce reactive oxygen species. Biochem. J. 417, 1–13. [PubMed: 19061483]

Naguib S, Backstrom JR, Gil M, Calkins DJ, Rex TS, 2021. Retinal oxidative stress activates the NRF2/ARE pathway: an early endogenous protective response to ocular hypertension. Redox Biol. 42, 101883, 101883. [PubMed: 33579667]

Nidhi K, Manisha T, Vikas P, Sandeep K, Sunil S, Ashok Kumar D, 2018. Oxidative stress: major threat in traumatic brain injury. CNS Neurol. Disord. - Drug Targets 17, 689–695. [PubMed: 29952272]

Nisenbaum EJ, Novikov DS, Lui YW, 2013. The presence and role of iron in mild traumatic brain injury: an imaging perspective. J. Neurotrauma 31, 301–307.

Nunomura A, Honda K, Takeda A, Hirai K, Zhu X, Smith MA, Perry G, 2006. Oxidative damage to RNA in neurodegenerative diseases. J. Biomed. Biotechnol. 82323, 82323.

Odhiambo WA, Guthua SW, Macigo FG, Akama MK, 2002. Maxillofacial injuries caused by terrorist bomb attack in Nairobi, Kenya. Int. J. Oral Maxillofac. Surg. 31, 374–377. [PubMed: 12361069]

Pacher P, Beckman JS, Liaudet L, 2007. Nitric oxide and peroxynitrite in health and disease. Physiol. Rev. 87, 315–424. [PubMed: 17237348]

Potter DR, Miyazawa BY, Gibb SL, Deng X, Togaratti PP, Croze RH, Srivastava AK, Trivedi A, Matthay M, Holcomb JB, Schreiber MA, Pati S, 2018. Mesenchymal stem cell-derived extracellular vesicles attenuate pulmonary vascular permeability and lung injury induced by hemorrhagic shock and trauma. J. trauma acute care surgery 84, 245–256.

Prevention, C.f.D.C.a, 2001. Rapid assessment of injuries among survivors of the terrorist attack on the World Trade Center–New York City. MMWR Morb. Mortal. Wkly. Rep. 51, 1–5.

Rasiah PK, Geier B, Jha KA, Gangaraju R, 2021. Visual Deficits after Traumatic Brain Injury. Histol Histopathol, p. 18315.

Rex TS, Tsui I, Hahn P, Maguire AM, Duan D, Bennett J, Dunaief JL, 2004. Adenovirus-mediated delivery of catalase to retinal pigment epithelial cells protects neighboring photoreceptors from photo-oxidative stress. Hum. Gene Ther. 15, 960–967. [PubMed: 15585111]

Scott MD, Wagner TC, Chiu DT, 1993. Decreased catalase activity is the underlying mechanism of oxidant susceptibility in glucose-6-phosphate dehydrogenase-deficient erythrocytes. Biochim. Biophys. Acta 1181, 163–168. [PubMed: 8481405]

Sen N, 2017. An insight into the vision impairment following traumatic brain injury. Neurochem. Int. 111, 103–107. [PubMed: 28163060]

Shimouchi A, Yokota H, Ono S, Matsumoto C, Tamai T, Takumi H, Narayanan SP, Kimura S, Kobayashi H, Caldwell RB, Nagaoka T, Yoshida A, 2016. Neuroprotective effect of water-dispersible hesperetin in retinal ischemia reperfusion injury. Jpn. J. Ophthalmol. 60, 51–61. [PubMed: 26407617]

Sies H, Jones DP, 2020. Reactive oxygen species (ROS) as pleiotropic physiological signalling agents. Nat. Rev. Mol. Cell Biol. 21, 363–383. [PubMed: 32231263]

Smith DH, Kochanek PM, Rosi S, Meyer R, Ferland-Beckham C, Prager EM, Ahlers ST, Crawford F, 2021. Roadmap for advancing pre-clinical science in traumatic brain injury. J. Neurotrauma, 0:null.

Vasquez-Vivar J, Shi Z, Jeong JW, Luo K, Sharma A, Thirugnanam K, Tan S, 2020. Neuronal vulnerability to fetal hypoxia-reoxygenation injury and motor deficit development relies on regional brain tetrahydrobiopterin levels. Redox Biol. 29, 101407. [PubMed: 31926630]

Vest V, Bernardo-Colón A, Watkins D, Kim B, Rex TS, 2019. Rapid repeat exposure to subthreshold trauma causes synergistic axonal damage and functional deficits in the visual pathway in a mouse model. J. Neurotrauma 36, 1646–1654. [PubMed: 30451083]

Xiong Y, Mahmood A, Chopp M, 2013. Animal models of traumatic brain injury. Nat. Rev. Neurosci. 14, 128–142. [PubMed: 23329160]

Yonekawa Y, Hacker HD, Lehman RE, Beal CJ, Veldman PB, Vyas NM, Shah AS, Wu D, Eliott D, Gardiner MF, Kuperwaser MC, Rosa RH Jr., Ramsey JE, Miller JW, Mazzoli RA, Lawrence MG, Arroyo JG, 2014. Ocular blast injuries in mass-casualty incidents: the marathon bombing in Boston, Massachusetts, and the fertilizer plant explosion in West, Texas. Ophthalmology 121, 1670–1676 e1671. [PubMed: 24841363]

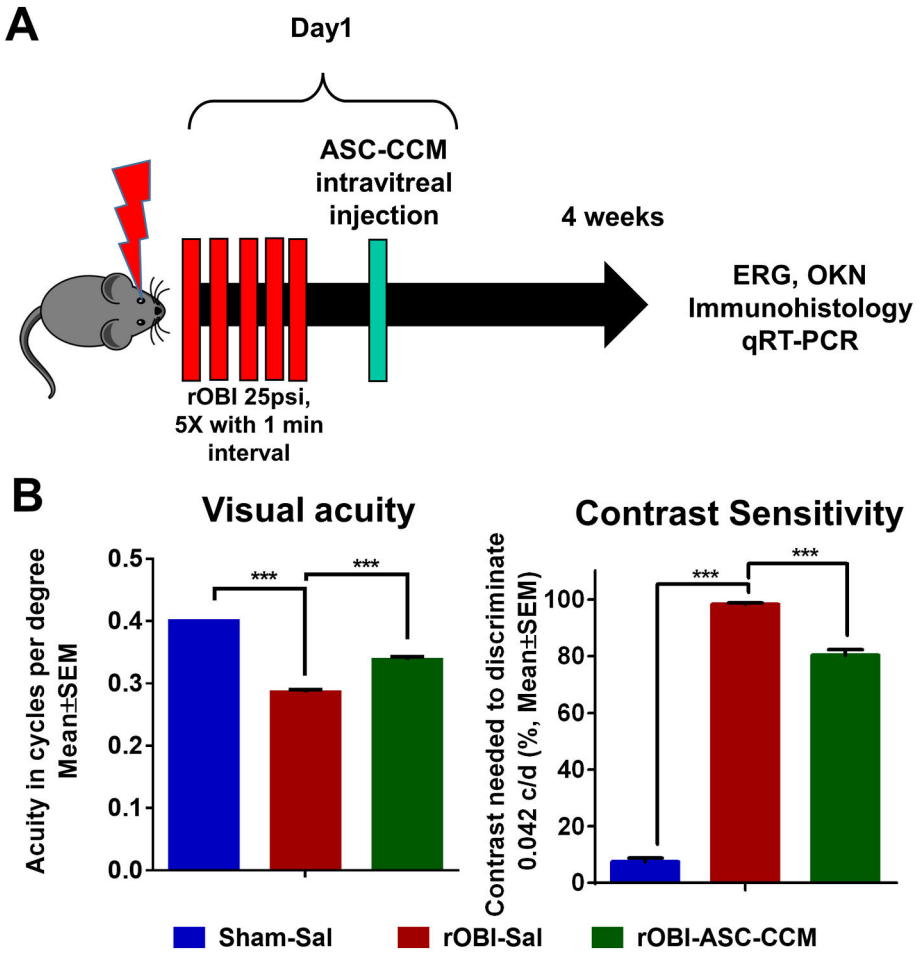

Fig. 1. ASC-CCM improves visual acuity and contrast sensitivity in rOBI mice.

(A): Timeline of rOBI mouse studies, intravitreal injection of ASC-CCM, and endpoint analyses. **(B):** Visual acuity and contrast sensitivity measurements in all groups of mice. Data represent combined Mean ± SEM from n = 7–11 animals/group. *, $p < 0.05$; ***, $p < 0.001$; #, $p > 0.05$.

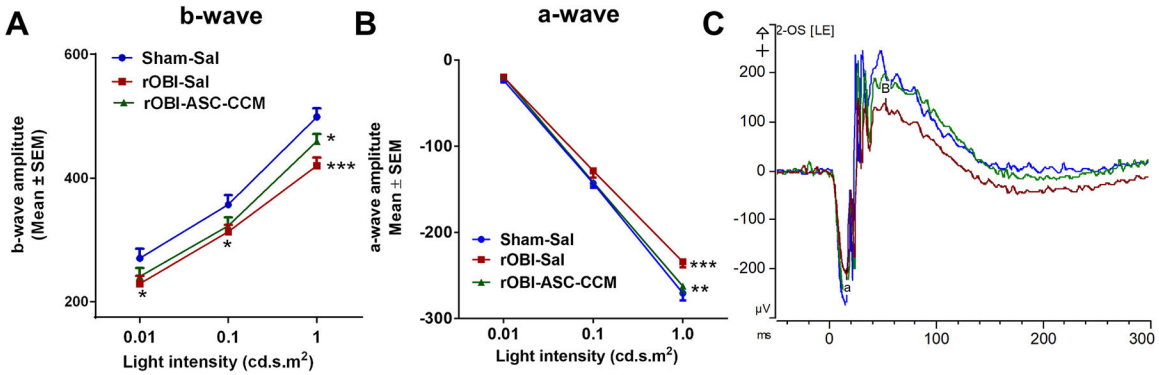

Fig. 2. ASC-CCM improves b-wave and a-wave amplitudes in rOBI mice.

(A): b-wave amplitude measurement in mice at various flash intensities in the injured eye. (**B**) a-wave amplitudes from the injured eye. (**C**) Representative electroretinogram tracings from each of the groups. Data represent combined Mean ± SEM from n = 7–11 animals/group. *, $p < 0.05$; **, $p < 0.01$; ***, $p < 0.001$.

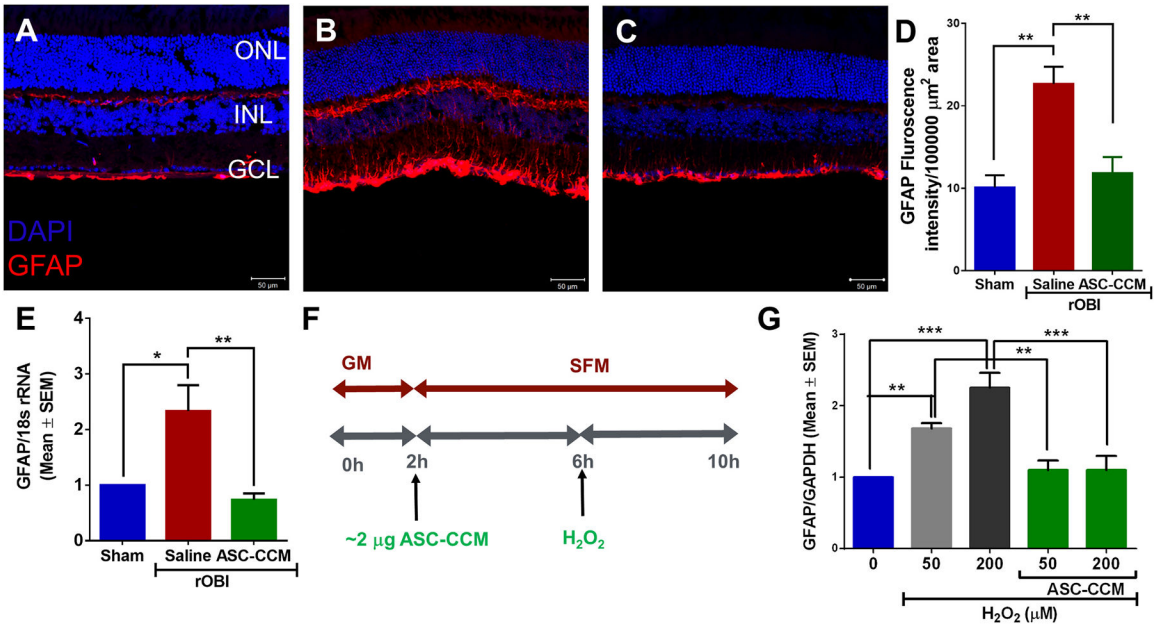

Fig. 3. ASC-CCM normalizes retinal GFAP expression in rOBI mice and in oxidative-stressed Müller cells *in vitro*.

Confocal microscope images of retinal tissue immunolabeled for GFAP in (**A**): Sham mice receiving saline, (**B**): rOBI mice receiving saline, and (**C**): rOBI mice receiving ASC-CCM. Scale bars for A-C = 50 μm. (**D**): Image J quantification of GFAP intensity in immunolabeled retinas. (**E**): mRNA quantification of mean retinal GFAP expression for all groups normalized to internal control (18s rRNA). Data in (D–E) represent Mean ± SEM from n = 4–6 animals/group. *, $p < 0.05$; **, $p < 0.01$. (**F**): Schematic representation of pretreatment of ASC-CCM and various doses of H_2O_2 exposure in rMC-1. (**G**): GFAP mRNA expression by TaqMan qPCR in rMC-1 cells and expressed as fold change normalized to internal control (GAPDH) in the experimental groups. Data represent Mean ± SEM from replicate measurements repeated independently.

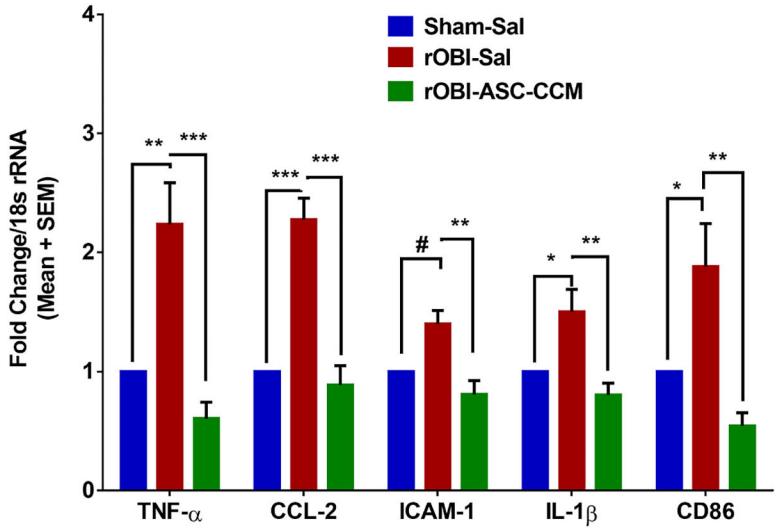

Fig. 4. ASC-CCM ameliorates pro-inflammatory (TNF-α, CCL2, and ICAM-1), and microglia/macrophage (CD86 and IL-1β) gene transcripts in rOBI mice.

Assessment of gene expression by TaqMan qPCR. Changes in target gene transcripts expressed as fold change normalized to internal control (18s rRNA) in the study groups. Data represent Mean ± SEM from $n = 3–5$ animals/group. *, $p < 0.05$; **, $p < 0.01$; ***, $p < 0.001$; #, $p > 0.05$.

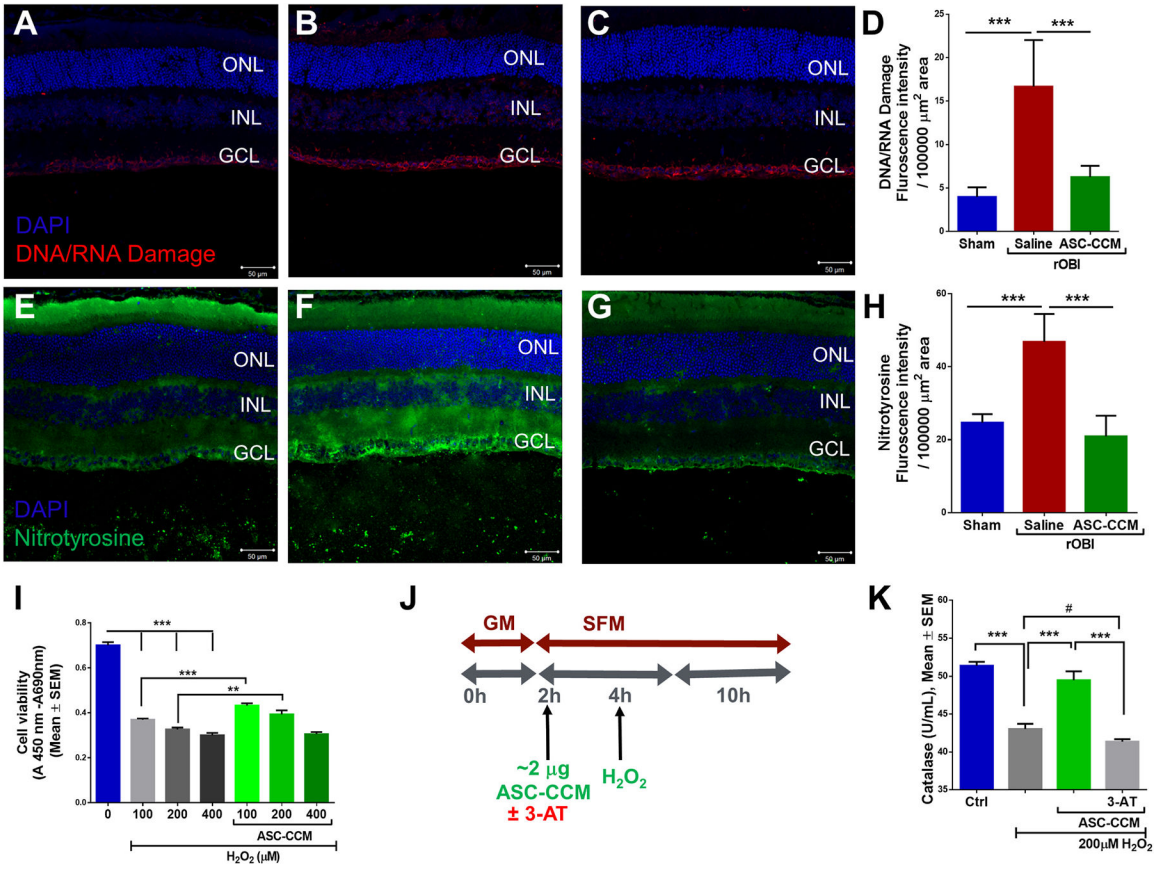

Fig. 5. ASC-CCM ameliorates increased oxidative stress in rOBI mice and decreased catalase activity in oxidatively stressed Müller cells *in vitro*.

Immunohistological analysis of retinal tissue for DNA/RNA damage marker antibody followed by confocal microscopy in (**A):** Sham mice recieveing saline (**B**): rOBI mice receiving saline, (**C**): rOBI mice receiving ASC-CCM, and (**D**): Image J quantification of DNA/RNA damage marker intensity for all groups. Immunohistological analysis of retinal tissue for anti-nitrotyrosine antibody followed by confocal microscopy in (**E):** Sham mice receiving saline (**F**): rOBI mice receiving saline, (**G**): rOBI mice receiving ASC-CCM, and (**H**): Image J quantification of anti-nitrotyrosine immunostaining intensity for all groups. Data in (D&H) represent Mean ± SEM from n = 4–6 animals/group. ***, $p < 0.001$. (**I**): Cell proliferation/viability was assessed with WST-1 Cell Proliferation Assay System in rMC-1 cells. (**J**): Schematic representation of pretreatment of ASC-CCM with 3-AT (0.5 mM of 3-Amino-1,2,4-triazole) and H_2O_2 exposure in rMC-1 for catalase activity assay. (**K**): Biochemical measurement of catalase activity in cell lysates from rMC-1 cells. Data represent Mean ± SEM from replicate measurements repeated independently. **, $p < 0.01$; ***, $p < 0.001$; #, $p > 0.05$.

Table 1

List of Taqman assay ID's for qPCR.

Gene	Assay ID	Reference
18S ribosomal RNA (*18S*)	Mm04277571	NR_003278.3
Tumor necrosis factor (*TNFα*)	Mm00443258_m1	NM_013693.3
Chemokine (C-C motif) ligand 2 (*CCL2*)	Mm00441242	NM_011333.3
Intercellular cell adhesion molecule 1 (*ICAM-1*)	Mm00516023_m1	NM_010493.2
Interleukin 1 β (*IL1β*)	Mm00434228_m1	NM_008361.3
Cluster of Differentiation 86 (*CD86*)	Mm00444543_m1	NM_019388.3
Glial fibric acid protein (*GFAP*)	Mm01253033_m1	NM_001131020.1
Glyceraldehydes 3-phosphate dehydrogenase (*GAPDH*)	Rn01462662_g1	NM_017008.4
Glial fibric acid protein (Rat *GFAP*)	Rn01253033_m1	NM_017009.2